Tianjin Daxue Xuebao (Ziran Kexue yu Gongcheng Jishu Ban)/
Journal of Tianjin University Science and Technology
ISSN (Online):0493-2137
E-Publication: Online Open Access
Vol: 59 Issue: 07:2026
DOI: 10.5281/zenodo.21412229

SYNERGISTIC REMINERALIZATION OF DEMINERALIZED ENAMEL BY SODIUM FLUORIDE AND ARGININE WITH BIOGENIC NANO B-TRICALCIUM PHOSPHATE: AN IN VITRO STUDY

SARA MUHAMAD SAMER ALASSABASHY*

Department of Pediatric and Preventive Dentistry and Dental Public Health, Faculty of Dentistry, Suez Canal University, 41522 Ismailia, Egypt. *Corresponding Author Email: salasbbashi@outlook.com

MOHAMED SHERIF MOHAMED SALAHELDIN FARAG

Department of Pediatric and Preventive Dentistry and Dental Public Health, Faculty of Dentistry, Suez Canal University, 41522 Ismailia, Egypt.

SABRY ABDELHAMEED ELKORASHY

Department of Inorganic Chemistry, Faculty of Science, Suez Canal University, 41522 Ismailia, Egypt.

Abstract

Introduction: Dental caries is a prevalent chronic oral disease in children, driven by cariogenic bacteria, frequent sugar intake, and poor oral hygiene. Early lesions can be managed noninvasively by remineralizing agents to prevent progression. Fluoride is effective but has dose-related limitations and may form surface barriers that impede subsurface remineralization. Aim: To compare the remineralizing effects of a 500 ppm sodium fluoride + 2% arginine solution with and without 1% nano biogenic β-tricalcium phosphate (β-TCP) derived from cuttlefish bone on demineralized premolar enamel. **Methods:** Seventy enamel halves from 35 premolars were allocated to five groups (n=14): Group I, sound enamel (control); Group II, demineralized; Group III, demineralized treated with 500 ppm NaF; Group IV, demineralized treated with 500 ppm NaF + 2% arginine; Group V, demineralized treated with 500 ppm NaF + 2% arginine + 1% nano β-TCP. Each group was split for surface microhardness (Vickers, n=7) and ESEM with EDX analysis (n=7). **Results:** Demineralization significantly reduced surface microhardness and Ca:P ratio. All treatments increased hardness and promoted surface repair; Group V achieved the greatest hardness recovery and the most enamel-like, dense morphology. Fluoride content increased in Groups IV and V versus Group III. Group V showed the highest Ca:P ratio, indicating superior mineral redeposition. **Conclusion:** Adding 1% nano biogenic β-TCP to a fluoride–arginine formulation enhanced remineralization of demineralized enamel more effectively than fluoride alone.

Keywords: Fluoride-Arginine Therapy, Nano β-Tricalcium Phosphate (Biogenic), Enamel Remineralization, Vickers Microhardness, Energy-Dispersive X-ray Analysis (EDX).

INTRODUCTION

Dental caries remains a prevalent chronic oral disease, disproportionately affecting pediatric populations and diminishing quality of life through pain, infection, and functional impairment (Bijl *et al.,* 2019). Caries develops from the interplay of cariogenic bacteria principally Streptococcus mutans-frequent dietary sugar exposure, and inadequate oral hygiene, which together create repeated acid challenges and net mineral loss from enamel (Bijl *et al.,* 2019). Early-stage, non-cavitated lesions can be managed noninvasively by remineralization therapies that promote mineral deposition and arrest lesion progression, thereby avoiding conventional invasive cavity preparation (Konagala *et al.,* 2020).

Tianjin Daxue Xuebao (Ziran Kexue yu Gongcheng Jishu Ban)/
Journal of Tianjin University Science and Technology
ISSN (Online):0493-2137
E-Publication: Online Open Access
Vol: 59 Issue: 07:2026
DOI: 10.5281/zenodo.21412229

Fluoride is the cornerstone of caries prevention due to its capacity to limit mineral loss, enhance remineralization, and form fluoro-apatite with increased acid resistance; nevertheless, excessive fluoride exposure carries risks such as dental and skeletal fluorosis and, in some contexts, may create a superficial hypermineralized layer that impedes deeper subsurface repair (Cheng *et al.,* 2015; Ten Cate and Buzalaf, 2019). Optimizing topical fluoride dosing is therefore essential to balance caries prevention against fluorosis risk, with age- and risk-adapted recommendations for smear- and pea-sized pastes in infants and young children, adult-strength formulations for older children, and professionally applied high-concentration varnishes or gels reserved for high-risk cases under clinician supervision (Dalal and Clark, 2019; Toumba *et al.,* 2019; Wong *et al.,* 2024). Acute and chronic fluoride toxicities ranging from gastrointestinal disturbances to dental and skeletal fluorosis further underscore the need for cautious exposure, particularly in pediatric and renally impaired populations (Kabir *et al.,* 2019; Nasiri *et al.,* 2021; Kashyap *et al.,* 2021; Cury *et al.,* 2019).

Adjunctive remineralizing agents that complement fluoride's mechanisms are attracting interest for their potential to enhance subsurface mineral recovery while minimizing fluoride-related risks. L-arginine, a semi-essential amino acid naturally present in saliva and dental plaque, is metabolized by arginolytic bacteria to produce ammonia, thereby raising plaque pH and favoring remineralization while inhibiting demineralization. Arginine can also complex with calcium and fluoride (Arg-Ca-F2), facilitating mineral penetration into porous enamel; combined arginine–fluoride formulations have demonstrated superior caries prevention and mineral gain compared with fluoride alone (Bijl *et al.,* 2019; Konagala *et al.,* 2020; Prasad *et al.,* 2023; Bijle *et al.,* 2018; Kuriki *et al.,* 2024; Bijle *et al.,* 2020). Supplementation with bioavailable calcium and phosphate is likewise important, since enamel recovery depends on local calcium/phosphate availability and plaque fluid Ca/P ratios are substantially lower than those of enamel (Arifa *et al.,* 2019).

β-Tricalcium phosphate (β-TCP) serves as a controlled-release source of calcium and phosphate that can synergize with fluoride to enhance remineralization, and recent work suggests that nano-scale, biogenic β-TCP derived from marine sources such as cuttlefish bone is a sustainable option with favorable in vitro effects on enamel morphology and microhardness (Seyedlar *et al.,* 2019; Hamba *et al.,* 2020; Limeback *et al.,* 2023; Pang *et al.,* 2024; Abd-elmonsif and Gamal, 2024). However, data are limited on the combined use of arginine–fluoride formulations with biogenic nano β-TCP.

This study therefore compares the remineralizing effect of a 500 ppm NaF + 2% arginine solution with and without 1% nano biogenic β-TCP synthesized from cuttlefish bone on demineralized premolar enamel. We tested the null hypothesis that no significant differences exist between the two formulations in restoring enamel surface hardness and mineral content. Characterizing synergistic strategies that combine fluoride, arginine, and bioavailable calcium phosphate may inform minimally invasive management of early carious lesions, particularly in vulnerable pediatric dentitions where enamel is thinner and more porous (Meyer *et al.,* 2022; Featherstone *et al.,* 2008).

Tianjin Daxue Xuebao (Ziran Kexue yu Gongcheng Jishu Ban)/
Journal of Tianjin University Science and Technology
ISSN (Online):0493-2137
E-Publication: Online Open Access
Vol: 59 Issue: 07:2026
DOI: 10.5281/zenodo.21412229

MATERIALS AND METHODS

This in vitro study evaluated the remineralizing effect of a 500 ppm sodium fluoride + 2% arginine treatment solution with or without 1% nano biogenic β-tricalcium phosphate (β-TCP) synthesized from cuttlefish bone on demineralized enamel. Thirty-five unidentified premolars extracted for orthodontic reasons were collected from the Outpatient Clinic of the Oral and Maxillofacial Surgery Department, Faculty of Dentistry, Suez Canal University. Experiments and materials characterization were performed at the Inorganic Chemistry Lab, Chemistry Department, Faculty of Science, Suez Canal University. The protocol was approved by the scientific committee of research (NO: 498/2024) and followed the Faculty of Dentistry's guidelines.

Study design and sample size:

This in vitro study used thirty-five sound premolars, sectioned mesiodistally along the central groove to yield 70 buccal and lingual halves. The total sample size of 70 was calculated according to the following equation:

$$f = \frac{\sigma_\mu}{\sigma}$$

$$\sigma_\mu^2 = \frac{\sum_{i=1}^{k} n_j (\mu_i - \mu)^2}{N}$$

f: is the effect size; α= 0.05; β=0.10; Power= 1- β = 0.90

Sample size of 70 was divided equally among five groups (n = 14 per group). Specimens were allocated by numbering 1–70 and randomizing group assignment using www.randomizer.org.

Inclusion criteria and specimen selection

Included teeth met criteria adapted from Gumus *et al.* (2020): sound enamel free of hypomineralization or hypoplasia, unrestored, and free of cracks or defects as confirmed by stereomicroscope inspection.

Grouping

Specimens were divided into five groups (n = 14 each; Table 1) and further into subgroups for surface microhardness (SMH) testing (Ia) and ESEM/EDX analysis (Ib):

Group I (control, normal enamel): Subgroups Ia and Ib.

Group II (demineralized): Subgroups Ia and Ib.

Group III (positive control): demineralized then treated with 500 ppm sodium fluoride.

Group IV: demineralized then treated with 500 ppm sodium fluoride + 2% arginine.

Group V: demineralized then treated with 500 ppm sodium fluoride + 2% arginine + 1% nano β-TCP.

Each group's specimens for SMH (Ia) and ESEM/EDX (Ib) comprised seven samples.

Tianjin Daxue Xuebao (Ziran Kexue yu Gongcheng Jishu Ban)/
Journal of Tianjin University Science and Technology
ISSN (Online):0493-2137
E-Publication: Online Open Access
Vol: 59 Issue: 07:2026
DOI: 10.5281/zenodo.21412229

Specimen preparation:

Teeth were cleaned with a #6/7 Zeffiro curette to remove calculus and polished with fluoride-free paste using a low-speed handpiece and soft brush (Aziz, 2021) (Fig. 1). Specimens were disinfected with 0.1% thymol for seven days and stored in normal saline at refrigerated temperature until use, with a maximum storage period of one month post-extraction (Abdslam *et al.,* 2022). Crowns were separated 2 mm below the cemento-enamel junction; roots discarded (Fig. 2). Crowns were sectioned vertically along the central groove using an ISOMET 4000 micro-saw (Buehler, USA) with a 0.6 mm disc at 2500 rpm and feed rate 10 mm/min under copious water coolant, producing 70 specimens (Fig. 3,4). Pulp tissue was removed with a spoon excavator.

Table (1): The total sample size calculations used in the study:

Groups	(ESEM) with (EDX)	Vicker test.	No. of samples
Group I	7	7	14
Group II	7	7	14
Group III	7	7	14
Group IV	7	7	14
Group V	7	7	14
Total sample size	35	35	70

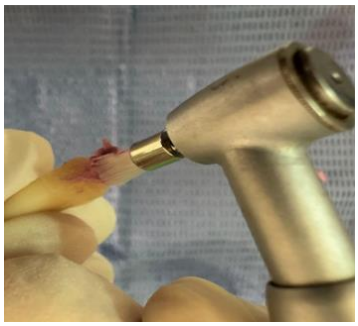

Fig 1a:Teeth cleaning

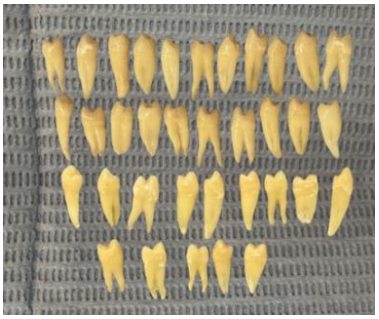

Fig 1b:All samples after cleaning

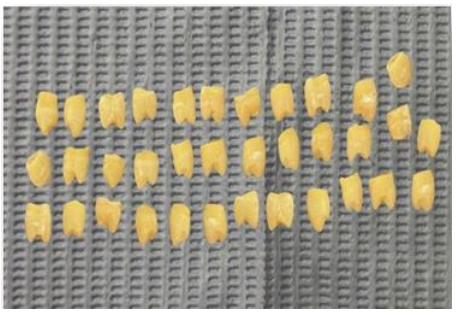

Fig 2: Crown- root separation

Fig 3: Isomet 4000 Micro Saw Buehler, USA

Tianjin Daxue Xuebao (Ziran Kexue yu Gongcheng Jishu Ban)/
Journal of Tianjin University Science and Technology
ISSN (Online):0493-2137
E-Publication: Online Open Access
Vol: 59 Issue: 07:2026
DOI: 10.5281/zenodo.21412229

Fig 4: Premolars after sectioning

Mounting for microhardness test:

For SMH testing, specimens were individually embedded in chemically cured acrylic resin (0.5 ml liquid:1 g powder mixed to dough consistency), placed centrally in a 13 mm diameter × ~8 mm high mold with the buccal or lingual surface parallel to the resin base (Hamdy, 2024) (Fig. 5-7). For ESEM/EDX, specimens were not embedded; instead they were fixed on separate glass plates with double-face tape (Fig. 8).

Fig 5: Samples individually fixed in self-cure acrylic resin

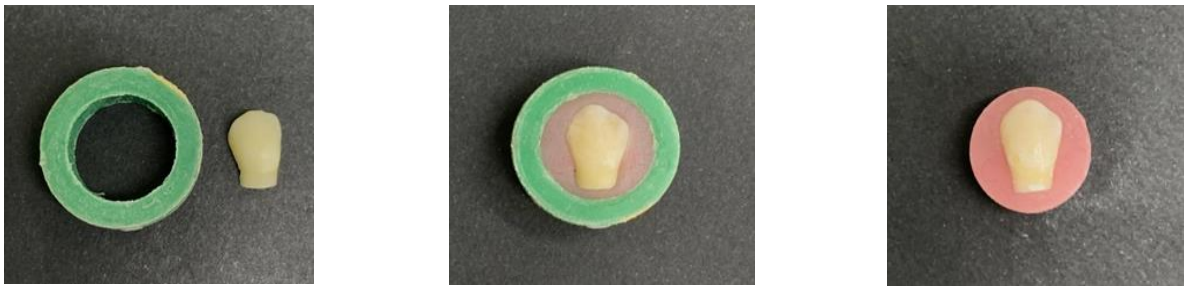

Fig 6: Steps of teeth mounting in the acrylic resin

Tianjin Daxue Xuebao (Ziran Kexue yu Gongcheng Jishu Ban)/
Journal of Tianjin University Science and Technology
ISSN (Online):0493-2137
E-Publication: Online Open Access
Vol: 59 Issue: 07:2026
DOI: 10.5281/zenodo.21412229

Fig 7: Diameter of acrylic base

Fig 8: Sample mounting for ESEM and EDX

Preparation and characterization of nano β-TCP

Biogenic nano β-TCP was synthesized from cuttlefish bone following Pang *et al.* (2024). Cuttlefish bone was washed, dried, crushed, ground, then thermally converted by heating at 900 °C for 5 h to convert calcium carbonate to calcium oxide. The powder was dispersed in deionized water and ultrasonicated for 10 min. Phosphoric acid was added dropwise with continuous stirring for 3 h, then subjected to hydrothermal treatment at 180 °C for 10 h. The solid phase was separated and calcined at 900 °C with a 10 °C/min heating rate, held for 2 h, then cooled at 20 °C/min to yield β-TCP nano-powders (Fig. 9-11). Characterization employed X-ray diffraction (XRD), Fourier transform infrared spectroscopy (FTIR), transmission electron microscopy (TEM), scanning electron microscopy (SEM) and EDX for phase identification, functional groups, particle size, morphology and elemental composition.

Fig 9: Cuttlefish bone after thorough cleaning and prior to the grinding process

Tianjin Daxue Xuebao (Ziran Kexue yu Gongcheng Jishu Ban)/
Journal of Tianjin University Science and Technology
ISSN (Online):0493-2137
E-Publication: Online Open Access
Vol: 59 Issue: 07:2026
DOI: 10.5281/zenodo.21412229

Fig 10: Preparation of biogenic β-TCP nano-powders

Fig 11: β-TCP nano-powder produced following hydrothermal treatment and calcination

Solutions and artificial caries formation

Demineralizing solution and artificial saliva compositions followed Mashhour *et al.* (2023) and Wierichs *et al.* (2018). The demineralizing solution contained 2.20 mM CaCl2, 2.20 mM monosodium phosphate, 1 M KOH and 0.05 M acetic acid (pH 4.4). Artificial saliva contained 1.5 mM CaCl2, 0.9 mM NaH2PO4 and 0.15 M KCl (pH 7.4). Artificial caries lesions were induced by immersing each specimen individually in 10 mL demineralizing solution for 96 h with daily solution replacement, followed by rinsing in deionized water (Fig. 12).

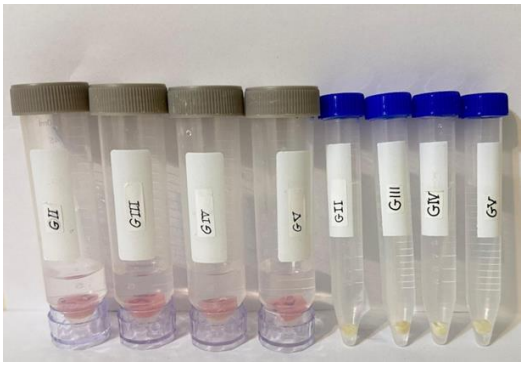

Fig 12: Samples immersion in demineralizing solution

Tianjin Daxue Xuebao (Ziran Kexue yu Gongcheng Jishu Ban)/
Journal of Tianjin University Science and Technology
ISSN (Online):0493-2137
E-Publication: Online Open Access
Vol: 59 Issue: 07:2026
DOI: 10.5281/zenodo.21412229

pH-cycling and remineralization protocol

Specimens underwent an 8-day pH-cycling regimen to simulate oral conditions (Queiroz *et al.,* 2008) (Fig. 13). Each 24-h cycle comprised 2 h in demineralizing solution and 22 h in artificial saliva at 37 °C. Three times daily (09:00, 14:00, 17:00), specimens were rinsed with distilled water then immersed for 5 min in their assigned freshly prepared remineralizing solution under agitation; 5 mL of remineralizing solution was used per exposure and replaced each time (Fig. 14,15). Solutions were renewed every 24 h.

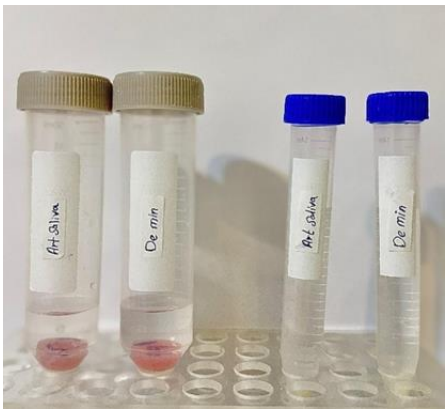

Fig 13: Tube containing artificial saliva and demineralizing solution

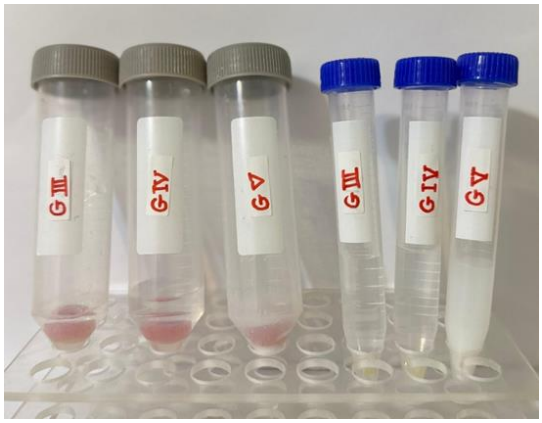

Fig 14: Tubes containing 3 different treatment solutions

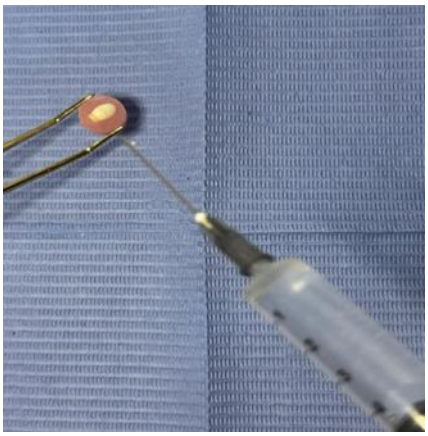

Fig 15: Washing samples with deionized water between each step

Evaluation methods

Surface microhardness (SMH): SMH was measured for subgroups Ia using a Vickers diamond indenter (Wilson TUKON 1102, Germany) with a 100 g load held for 10 s. Three indentations were made in incisal, middle and cervical thirds and averaged; a minimum 150 µm spacing was maintained between indentations (Salinovic *et al.,* 2021). Vickers hardness values were calculated as MHV = 1854.4L/d2.

Tianjin Daxue Xuebao (Ziran Kexue yu Gongcheng Jishu Ban)/
Journal of Tianjin University Science and Technology
ISSN (Online):0493-2137
E-Publication: Online Open Access
Vol: 59 Issue: 07:2026
DOI: 10.5281/zenodo.21412229

ESEM and EDX: Subgroup Ib specimens were air-dried for 2 h, mounted on aluminum stubs with double-sided tape and coded (Fig. 16). Samples were examined with an ESEM Prisma E (ThermoFisher) equipped with EDX at 30 kV at magnifications ×500, ×1000 and ×2000. Representative micrographs and EDX spectra provided ultrastructural morphology and weight percentages of Ca, P and F and Ca/P ratios to assess mineral changes (Hegde and Moany, 2012).

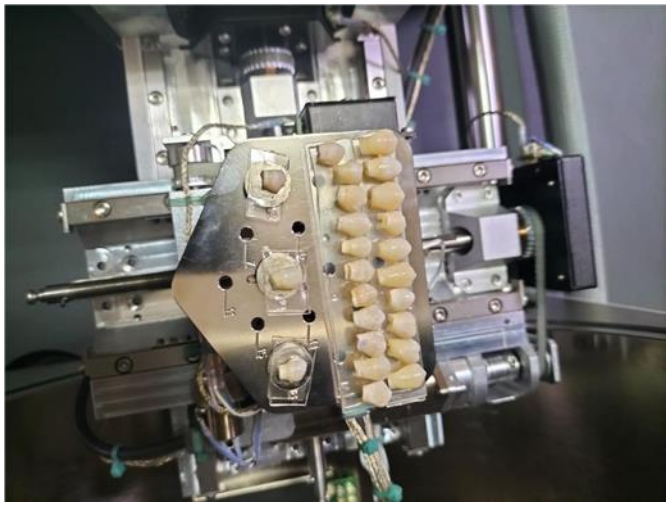

Fig 16: Teeth specimens fixed for ESEM and EDX analysis

Statistical analysis

Data normality was assessed with Shapiro–Wilk. Descriptive statistics are reported as mean ± SD. Group comparisons employed one-way ANOVA with Bonferroni post hoc pairwise tests; significance was set at $P \leq 0.05$. Statistical analyses were performed using SPSS for Windows version 26.0 (IBM Corp).

RESULTS

Thirty-five extracted premolars were used to evaluate the remineralizing effect of a 500 ppm sodium fluoride + 2% arginine solution with or without 1% nano biogenic β-tricalcium phosphate (β-TCP) synthesized from cuttlefish bone. Outcomes included characterization of the synthesized β-TCP, enamel surface microhardness (Vickers test), surface morphology (Environmental Scanning Electron Microscopy, ESEM), and elemental composition (Energy Dispersive X-ray spectroscopy, EDX). Results are presented in four parts.

I. Characterization of biogenic nano β-TCP derived from cuttlefish bone

X-Ray Diffraction (XRD) analysis demonstrated that β-TCP samples prepared at 900 °C produced diffraction patterns matching the standard β-TCP pattern reported by Madhukumar *et al.* (2007), corresponding to XRD card no. 00-009-0169 (Fig. 17). Fourier Transform Infrared Spectroscopy (FTIR) of the synthesized powder revealed

Tianjin Daxue Xuebao (Ziran Kexue yu Gongcheng Jishu Ban)/
Journal of Tianjin University Science and Technology
ISSN (Online):0493-2137
E-Publication: Online Open Access
Vol: 59 Issue: 07:2026
DOI: 10.5281/zenodo.21412229

characteristic phosphate absorption bands at 1021, 603, and 553 cm−1, consistent with previous reports (Mehdikhani and Borhani, 2014) (Fig. 18). Transmission Electron Microscopy (TEM) images indicated nanoparticles with an average diameter of ~33 nm (Fig. 19). Scanning Electron Microscopy (SEM) showed agglomerated, irregularly shaped particles (Fig. 20) and EDX elemental analysis confirmed the presence of O, P, C, and Ca with weight percentages of 18.2, 23.2, 6.9, and 51.7, respectively, in agreement with literature (Al-Qahtani *et al.,* 2022) (Fig. 20).

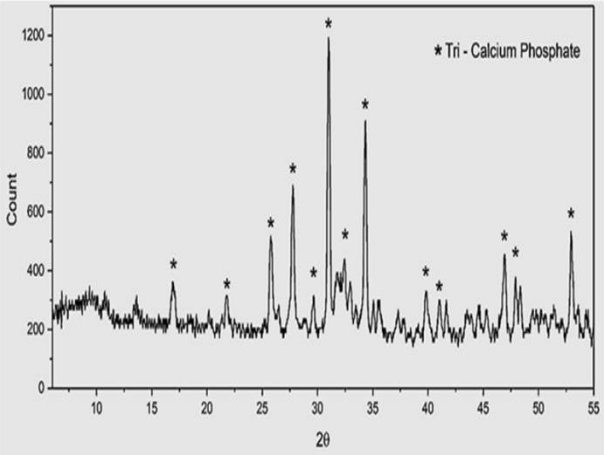

Fig 17: XRD of synthesized nano β-TCP derived from cuttlefish bone

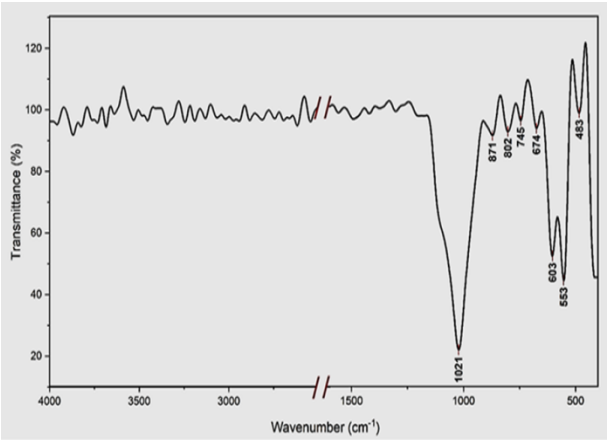

Fig 18: FTIR of synthesized nano β-TCP

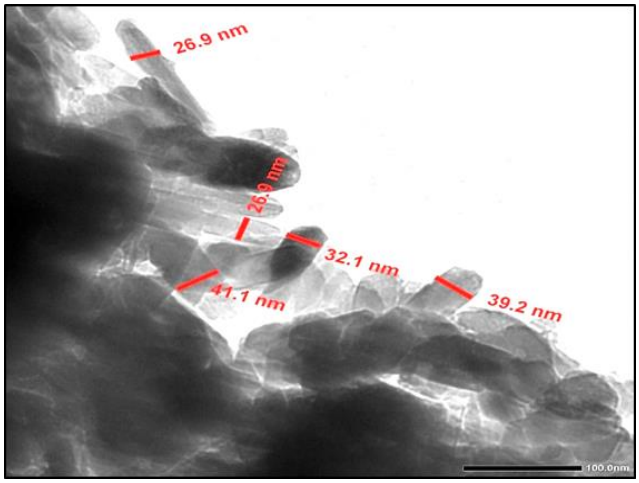

Fig 19: TEM micrograph for nano β-TCP prepared from cuttlefish bone showing nanoparticles with an average size of approximately 33 nm

Tianjin Daxue Xuebao (Ziran Kexue yu Gongcheng Jishu Ban)/
Journal of Tianjin University Science and Technology
ISSN (Online):0493-2137
E-Publication: Online Open Access
Vol: 59 Issue: 07:2026
DOI: 10.5281/zenodo.21412229

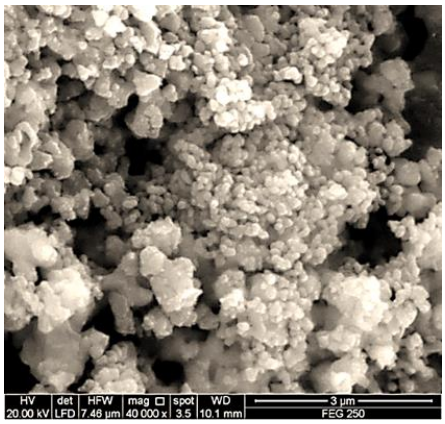

Fig 20 (a): SEM of β-TCP

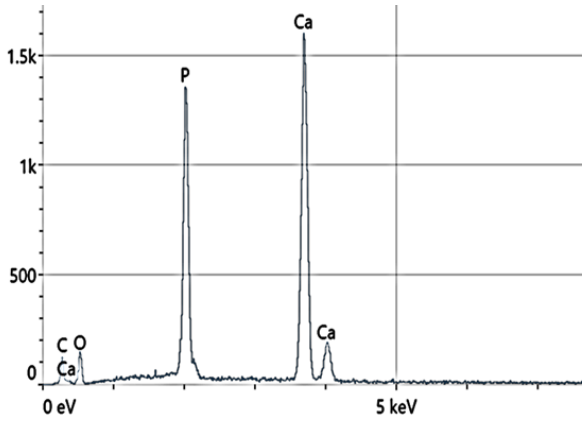

Fig 20 (b): Graph representing EDX spectra of β-TCP

II. Microhardness test results (Vickers test)

Vickers microhardness testing revealed significant differences across the five experimental groups (GI–GV), with a highly significant one-way ANOVA ($F=17.973$, $P<0.001$). Mean Vickers hardness numbers (VHN) ranked as follows: GI (negative control, sound enamel) highest at 281.60, GV (500 ppm NaF + 2% arginine + 1% β-TCP) at 239.80, GIV (500 ppm NaF + 2% arginine) at 227.20, GIII (500 ppm NaF) at 204.40, and GII (demineralized) lowest at 178.40 (Table 2, Fig. 21). Bonferroni post hoc pairwise comparisons (denoted by letters a, b, c, d) identified statistically distinct clusters; groups that share the same letter are not significantly different ($P<0.05$). Overall, GI showed the greatest hardness and GII the lowest, while GV, GIV, and GIII occupied intermediate positions with some overlaps in statistical similarity.

III. Environmental Scanning Electron Microscopy (ESEM) observations

ESEM imaging provided morphological corroboration of the microhardness data.

Group I (negative control): Enamel surfaces appeared smooth, compact, and homogeneous with well-organized, densely packed prisms and faint continuous prism outlines, representing intact enamel morphology (Fig. 22-24).

Group II (demineralized): ESEM revealed marked surface deterioration with exposed prism cores, widened interprismatic spaces, increased surface roughness and porosity, and an etching honeycomb-like pattern indicative of acid-induced demineralization (Fig. 25-27).

Group III (500 ppm NaF): Treated surfaces showed partial recovery relative to GII, with a relatively uniform and more compact appearance, reduced porosity, and globular/fused granular deposits consistent with fluoride-induced precipitation (fluorapatite-like), though complete remineralization was not achieved (Fig. 28-30).

Tianjin Daxue Xuebao (Ziran Kexue yu Gongcheng Jishu Ban)/
Journal of Tianjin University Science and Technology
ISSN (Online):0493-2137
E-Publication: Online Open Access
Vol: 59 Issue: 07:2026
DOI: 10.5281/zenodo.21412229

Table (2): Comparison between microhardness values of the five groups with means and standard deviations (±SD)

Group	Mean	SD	F test	P value
GI	281.60[a]	25.57	17.973	<0.001**
GII	178.40[d]	38.27		
GIII	204.40[cd]	15.67		
GIV	227.20[bc]	16.48		
GV	239.80[b]	17.11		
Pairwise comparison using Bonferroni post hoc				
Pairwise	**difference**	**P value**		
GI vs GII	103.20	<0.001**		
GI vs GIII	77.20	<0.001**		
GI vs GIV	54.40	<0.001**		
GI vs GV	41.80	0.003*		
GII vs GIII	-26.00	0.054		
GII vs GIV	-48.80	0.001*		
GII vs GV	-61.40	<0.001**		
GIII vs GIV	-22.80	0.088		
GIII vs GV	-35.40	0.010*		
GIV vs GV	-12.60	0.338		

Different superscript letters mean significant at P<0.05

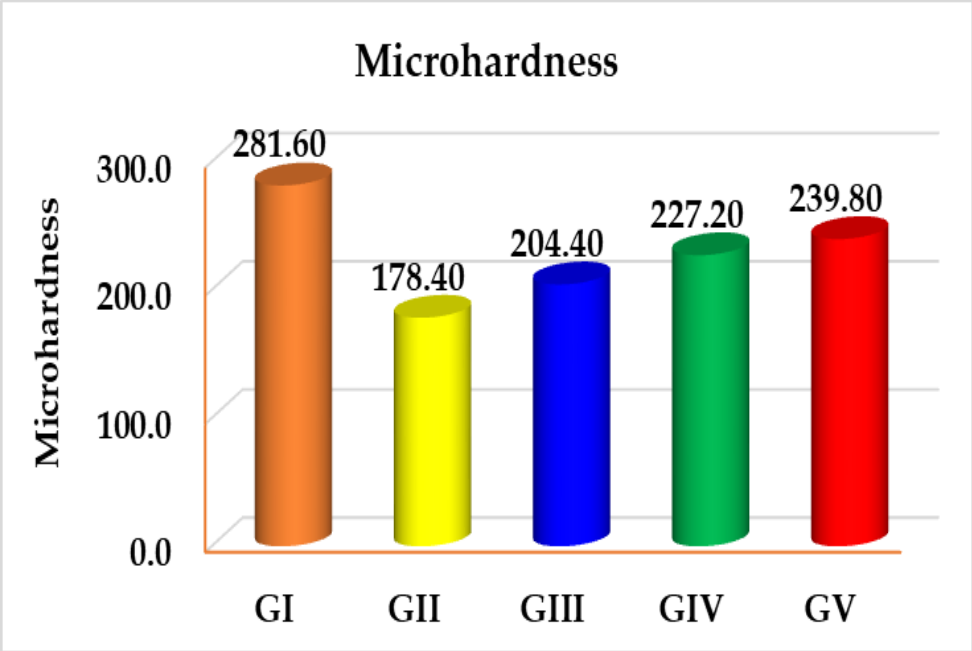

Fig 21: Bar chart representing mean values for microhardness of the five groups

Tianjin Daxue Xuebao (Ziran Kexue yu Gongcheng Jishu Ban)/
Journal of Tianjin University Science and Technology
ISSN (Online):0493-2137
E-Publication: Online Open Access
Vol: 59 Issue: 07:2026
DOI: 10.5281/zenodo.21412229

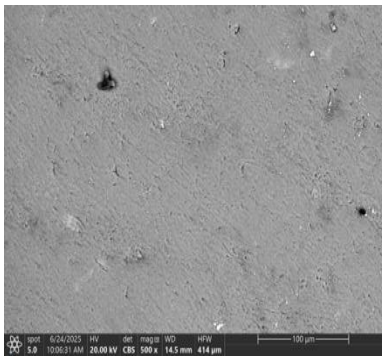

Fig 22: Scanning electron micrograph of sound enamel with overall smooth and compact surface and no visible porosities or surface irregularities, (X500)

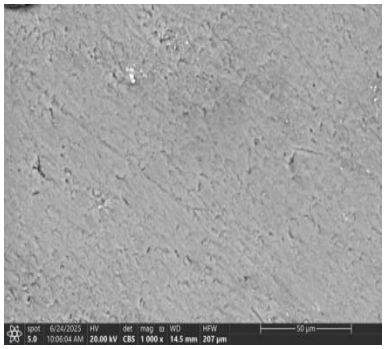

Fig 23: Scanning electron micrograph at higher magnification, the enamel prisms appear well-organized and tightly packed, indicating an intact and highly mineralized structure, (X1000)

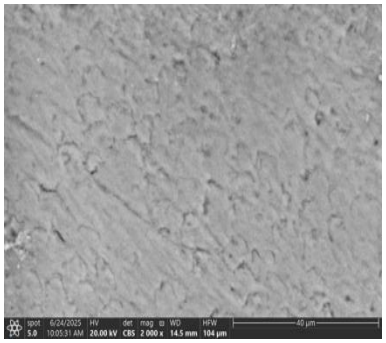

Fig 24: Scanning electron micrograph at high magnification with a dense, homogeneous crystalline surface, minimal microdefects, and continuous prism boundaries, characteristic of healthy enamel, (X2000)

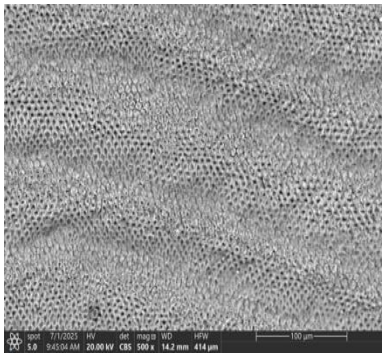

Fig 25: Scanning electron micrograph with a rough and uneven enamel surface with visible porosity following the demineralization process, (X500)

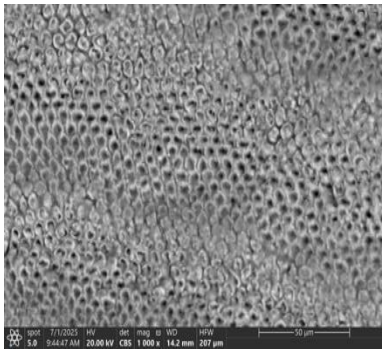

Fig 26: Scanning electron micrograph with distinct prism outlines and widened interprismatic spaces, indicating dissolution of enamel minerals and surface breakdown, (X1000)

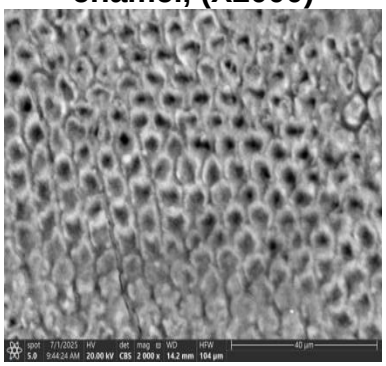

Fig 27: Scanning electron micrograph at higher magnification, the surface exhibits a pronounced honeycomb-like appearance, with exposed prism cores and irregular etching typical of demineralized enamel, (X2000)

Tianjin Daxue Xuebao (Ziran Kexue yu Gongcheng Jishu Ban)/
Journal of Tianjin University Science and Technology
ISSN (Online):0493-2137
E-Publication: Online Open Access
Vol: 59 Issue: 07:2026
DOI: 10.5281/zenodo.21412229

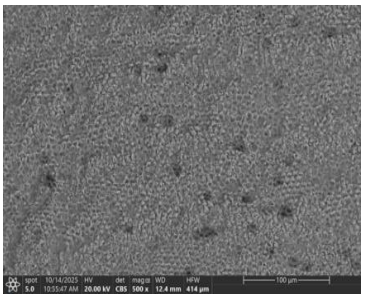

Fig 28: Scanning electron micrograph with partial surface smoothening and reduction in surface roughness compared to the demineralized enamel, (X500)

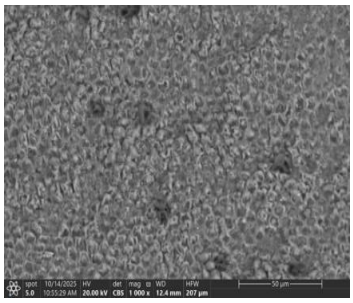

Fig 29: Scanning electron micrograph with evidence of mineral deposition, partial occlusion of prism cores, and decreased porosity, (X1000)

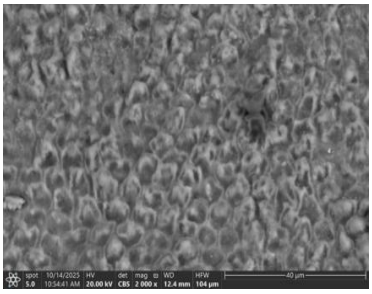

Fig 30: Scanning electron micrograph at higher magnification with localized mineral clusters covering some prism areas, indicating partial remineralization induced by fluoride treatment, (X2000)

Group IV (500 ppm NaF + 2% arginine): Surfaces displayed a smoother and more uniform layer than GIII, featuring dense fused globular deposits and effective occlusion of most microporosities. The morphology suggested enhanced surface mineralization compared with fluoride alone, consistent with a synergistic effect of arginine and fluoride (Fig. 31-33).

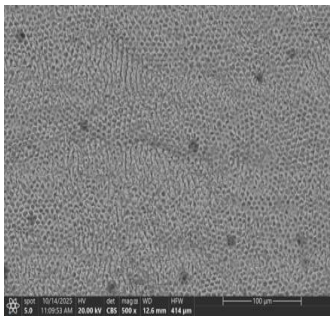

Fig 31: Scanning electron micrograph with smoother and more homogeneous surface compared to fluoride-only treatment, indicating improved remineralization, (X500)

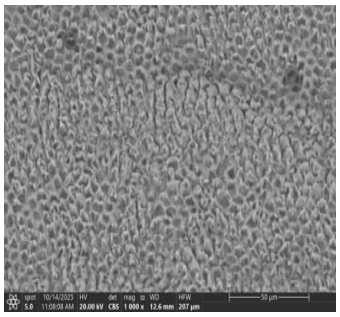

Fig 32: Scanning electron micrograph with uniform mineral deposits, suggesting surface repair and reprecipitation of minerals, (X1000)

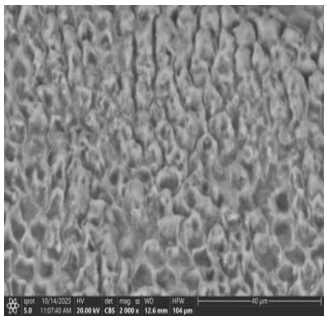

Fig 33: Scanning electron micrograph at high magnification, the surface appears compact with mineral-rich deposits bridging interprismatic areas (X2000)

Group V (500 ppm NaF + 2% arginine + 1% β-TCP):

ESEM showed the most advanced remineralization, with a compact, continuous mineralized surface, nearly complete coverage of enamel prisms, fused densely packed

Tianjin Daxue Xuebao (Ziran Kexue yu Gongcheng Jishu Ban)/
Journal of Tianjin University Science and Technology
ISSN (Online):0493-2137
E-Publication: Online Open Access
Vol: 59 Issue: 07:2026
DOI: 10.5281/zenodo.21412229

mineral deposits, and minimal residual porosity. This group exhibited the most uniform and dense mineral deposition among all groups (Fig. 34-36).

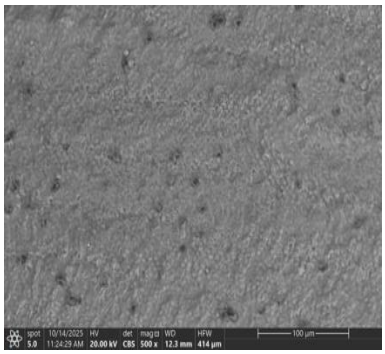

Fig 34: Scanning electron micrograph with markedly smooth and dense enamel surface with minimal irregularities, suggesting effective surface recovery, (X500)

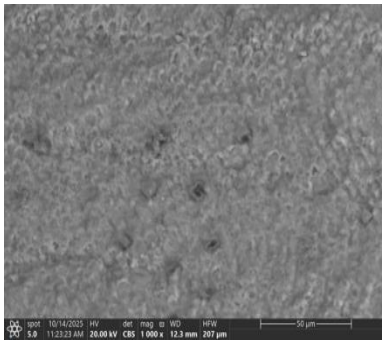

Fig 35: Scanning electron micrograph with enamel prisms almost completely occluded with newly deposited minerals, forming a uniform surface layer, (X1000)

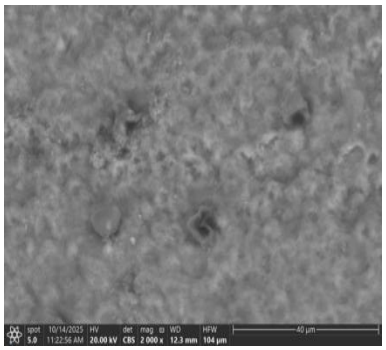

Fig 36: Scanning electron micrograph at higher magnification, the enamel shows a compact, continuous mineral layer with nearly complete closure of interprismatic spaces, (X2000)

IV. Energy Dispersive X-ray spectroscopy (EDX) elemental composition:

EDX spectra (Fig. 37-41) were analyzed for weight% of calcium (Ca), phosphorus (P), fluoride (F), and calculated Ca/P ratios. One-way ANOVA results and Bonferroni post hoc tests identified statistically distinct clusters as follows.

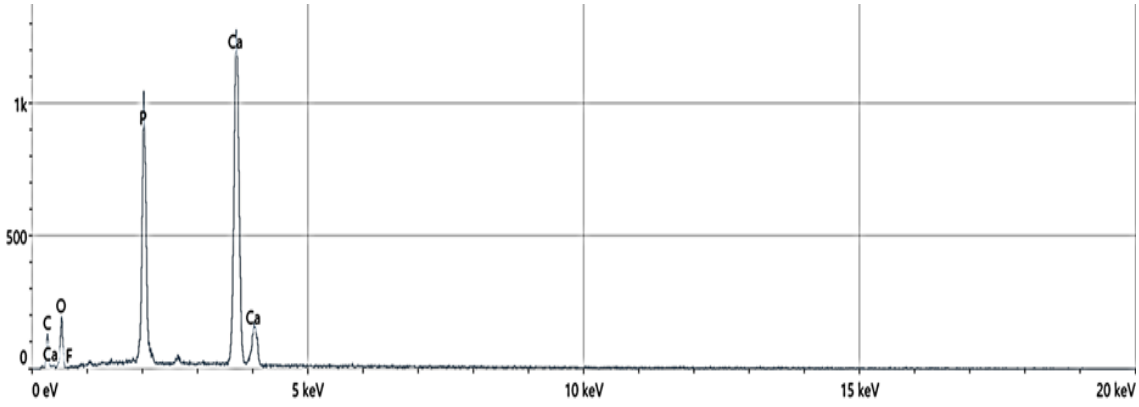

Fig 37: Graph representing EDX spectra of a tooth sample in group I

Tianjin Daxue Xuebao (Ziran Kexue yu Gongcheng Jishu Ban)/
Journal of Tianjin University Science and Technology
ISSN (Online):0493-2137
E-Publication: Online Open Access
Vol: 59 Issue: 07:2026
DOI: 10.5281/zenodo.21412229

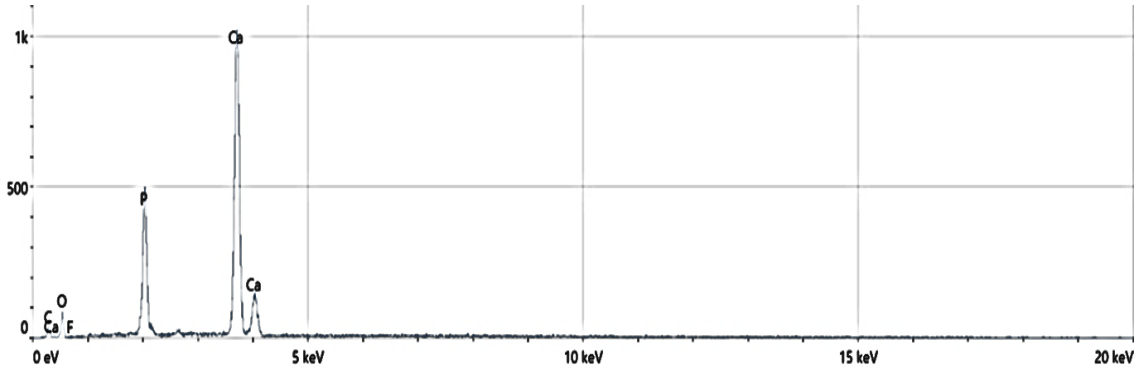

Fig 38: Graph representing EDX spectra of a tooth sample in group II

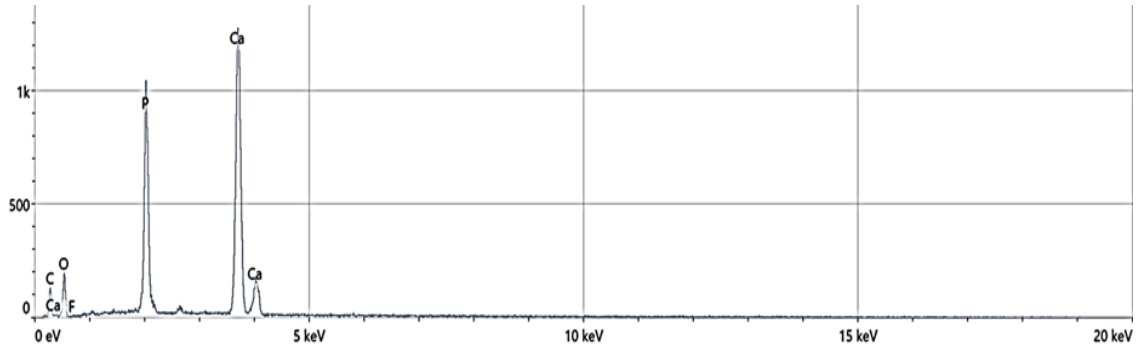

Fig 39: Graph representing EDX spectra of a tooth sample in group III

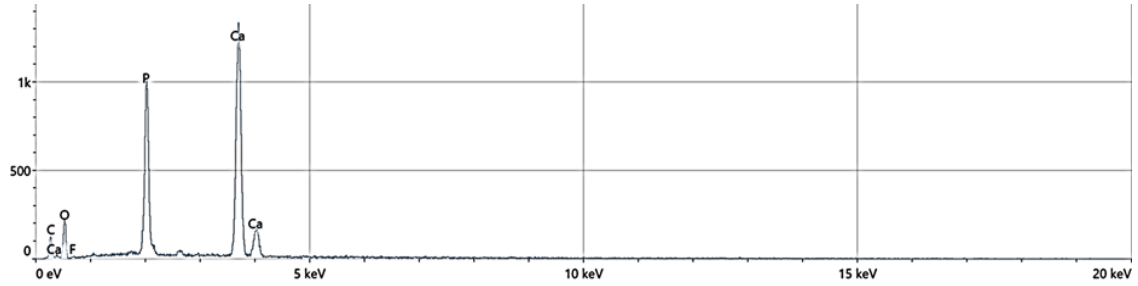

Fig 40: Graph representing EDX spectra of a tooth sample in group IV

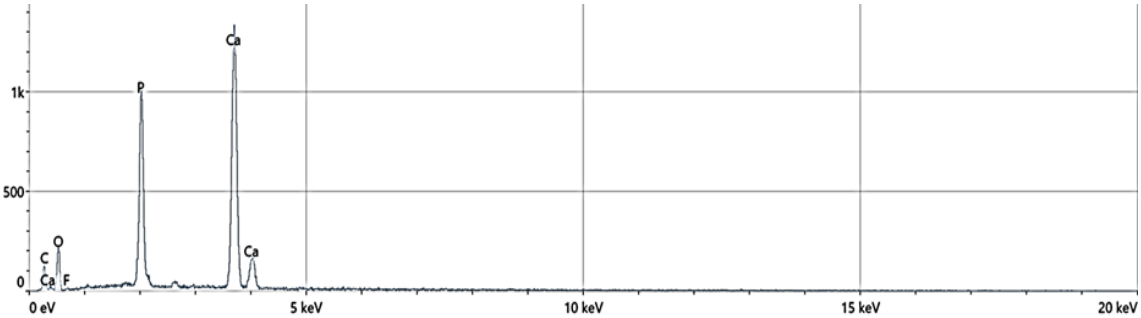

Fig 41: Graph representing EDX spectra of a tooth sample in group V

Tianjin Daxue Xuebao (Ziran Kexue yu Gongcheng Jishu Ban)/
Journal of Tianjin University Science and Technology
ISSN (Online):0493-2137
E-Publication: Online Open Access
Vol: 59 Issue: 07:2026
DOI: 10.5281/zenodo.21412229

Calcium (Ca) weight%: Significant differences were observed among groups (F = 93.861, P < 0.001). GI (47.73) and GV (46.81) had the highest Ca content and were statistically similar; GIII (37.19) and GIV (37.53) shared an intermediate cluster; GII (34.39) was lowest and statistically different from all others (Table 3, Fig. 42). Thus three clusters emerged: high (GI, GV), intermediate (GIII, GIV), and low (GII).

Table (3): Comparison between mean value and standard deviation of Ca weight % of the five groups with means and standard deviations (±SD)

Group	Mean	SD	F test	P value
GI	47.73 [a]	2.53	93.861	<0.001**
GII	34.39 [c]	1.30		
GIII	37.19[b]	1.03		
GIV	37.53[b]	1.43		
GV	46.81[a]	1.64		
Pairwise comparison using Bonferroni post hoc				
Pairwise	**difference**	**P value**		
GI vs GII	13.34	<0.001**		
GI vs GIII	10.54	<0.001**		
GI vs GIV	10.20	<0.001**		
GI vs GV	0.91	0.313		
GII vs GIII	-2.80	0.004*		
GII vs GIV	-3.14	0.001*		
GII vs GV	-12.43	<0.001**		
GIII vs GIV	-0.34	0.703		
GIII vs GV	-9.63	<0.001**		
GIV vs GV	-9.29	<0.001**		

Different superscript letters mean significant at P<0.05

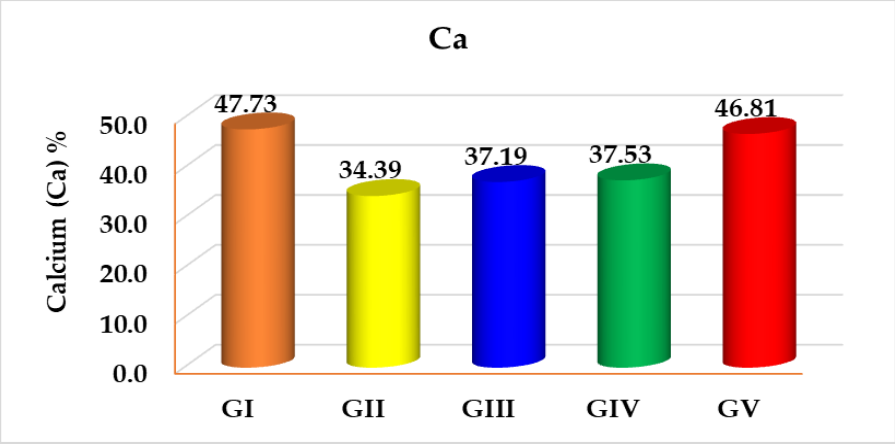

Fig 42: Bar chart representing mean values for Ca weight % of five groups

Phosphorus (P) weight%: ANOVA indicated significant differences (F = 12.376, P < 0.001). GI (19.24) and GV (18.94) had the highest P and were similar; GII (17.16), GIII

Tianjin Daxue Xuebao (Ziran Kexue yu Gongcheng Jishu Ban)/
Journal of Tianjin University Science and Technology
ISSN (Online):0493-2137
E-Publication: Online Open Access
Vol: 59 Issue: 07:2026
DOI: 10.5281/zenodo.21412229

(17.36), and GIV (17.33) formed a lower cluster with no significant differences among them (Table 4, Fig. 43). The data separate into high-P (GI, GV) and low-P (GII, GIII, GIV) groups.

Table (4): Comparison between mean value and standard deviation of P weight % of the five groups with means and standard deviations (±SD)

Group	Mean	SD	F test	P value
GI	19.24[a]	0.41	12.376	<0.001**
GII	17.16[b]	1.06		
GIII	17.36[b]	0.96		
GIV	17.33[b]	0.57		
GV	18.94[a]	0.53		
Pairwise comparison using Bonferroni post hoc				
Pairwise	**difference**	**P value**		
GI vs GII	2.09	<0.001**		
GI vs GIII	1.89	<0.001**		
GI vs GIV	1.91	<0.001**		
GI vs GV	0.30	0.462		
GII vs GIII	-0.20	0.623		
GII vs GIV	-0.17	0.673		
GII vs GV	-1.79	<0.001**		
GIII vs GIV	0.03	0.944		
GIII vs GV	-1.59	<0.001**		
GIV vs GV	-1.61	<0.001**		

Different superscript letters mean significant at P<0.05

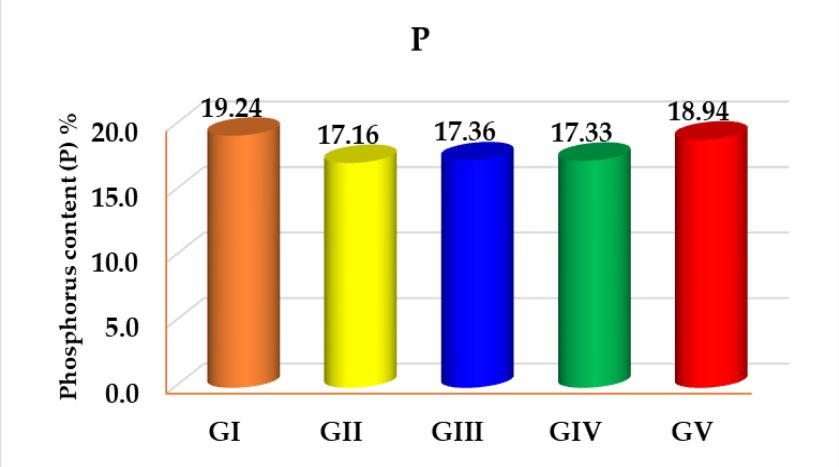

Fig 43: Bar chart representing mean values for P weight % of the five groups

Fluoride (F) weight%: Significant group differences were found (F = 16.515, P < 0.001). Highest F levels occurred in GV (1.50) and GIV (1.43), which were statistically similar (letter a). GIII (0.97) was intermediate (letter b), while GI (0.46) and GII (0.11) had the

Tianjin Daxue Xuebao (Ziran Kexue yu Gongcheng Jishu Ban)/
Journal of Tianjin University Science and Technology
ISSN (Online):0493-2137
E-Publication: Online Open Access
Vol: 59 Issue: 07:2026
DOI: 10.5281/zenodo.21412229

lowest and were statistically similar (letter c) (Table 5, Fig. 44). Ranking: GV/GIV > GIII > GI/GII.

Table (5): Comparison between mean value and standard deviation of F weight % of the five groups with means and standard deviations (±SD)

Group	Mean	SD	F test	P value
GI	0.46[c]	0.38	16.515	<0.001**
GII	0.11[c]	0.19		
GIII	0.97[b]	0.35		
GIV	1.43[a]	0.52		
GV	1.50[a]	0.44		
Pairwise comparison using Bonferroni post hoc				
Pairwise	**difference**	**P value**		
GI vs GII	0.34	0.113		
GI vs GIII	-0.51	0.020**		
GI vs GIV	-0.97	0.001**		
GI vs GV	-1.04	0.001**		
GII vs GIII	-0.86	0.001**		
GII vs GIV	-1.31	0.001**		
GII vs GV	-1.39	0.001**		
GIII vs GIV	-0.46	0.038		
GIII vs GV	-0.53	0.017**		
GIV vs GV	-0.07	0.736		

Different superscript letters mean significant at P<0.05

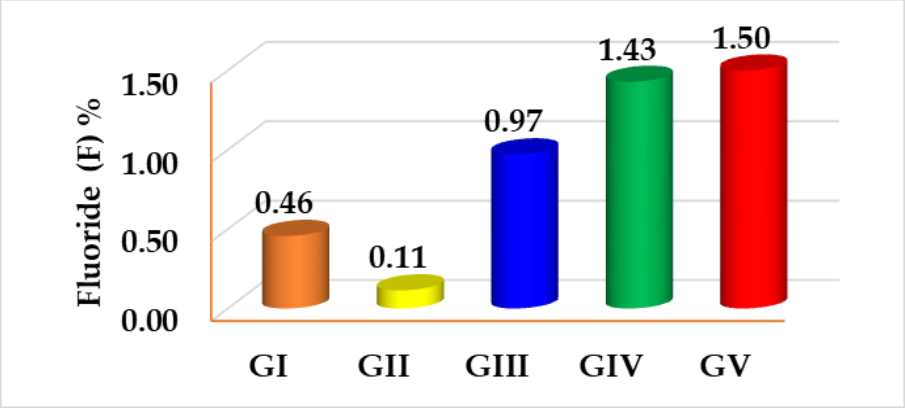

Fig 44: Bar chart representing mean values for F weight % of five groups

Ca/P ratio: Significant differences were present (F = 20.601, P < 0.001). GI (2.48) and GV (2.47) had the highest and were similar, whereas GII (2.01), GIII (2.15), and GIV (2.17) formed a lower cluster with no significant intergroup differences (Table 6, Fig. 45). GI and GV showed significantly higher Ca/P ratios than the remaining groups.

Tianjin Daxue Xuebao (Ziran Kexue yu Gongcheng Jishu Ban)/
Journal of Tianjin University Science and Technology
ISSN (Online):0493-2137
E-Publication: Online Open Access
Vol: 59 Issue: 07:2026
DOI: 10.5281/zenodo.21412229

Table (6): Comparison between mean and standard deviation value of Ca/P weight ratio of the five groups with means and standard deviations (±SD)

Group	Mean	SD	F test	P value
GI	2.48[a]	0.12	20.601	<0.001**
GII	2.01[b]	0.16		
GIII	2.15[b]	0.12		
GIV	2.17[b]	0.11		
GV	2.47[a]	0.08		
Pairwise comparison using Bonferroni post hoc				
Pairwise	**difference**	**P value**		
GI vs GII	0.47	<0.001**		
GI vs GIII	0.33	<0.001**		
GI vs GIV	0.31	<0.001**		
GI vs GV	0.01	0.897		
GII vs GIII	-0.14	0.045*		
GII vs GIV	-0.16	0.022**		
GII vs GV	-0.46	<0.001**		
GIII vs GIV	-0.02	0.747		
GIII vs GV	-0.33	<0.001**		
GIV vs GV	-0.30	<0.001**		

Different superscript letters mean significant at P<0.05

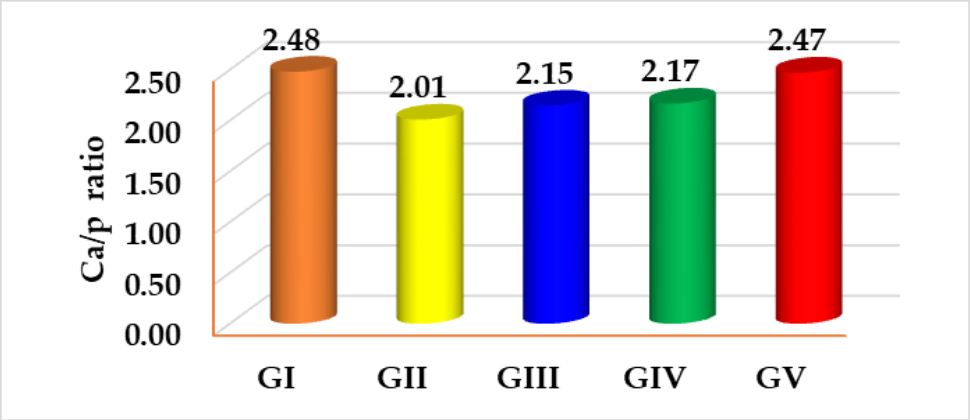

Fig 45: Bar chart representing mean values for Ca/P weight ratio% of five groups

DISCUSSION

The present in vitro study evaluated the remineralizing efficacy of a 500 ppm sodium fluoride (NaF) + 2% arginine solution with and without 1% biogenic nano β-tricalcium phosphate (β-TCP) (derived from cuttlefish bone) on artificially demineralized human premolar enamel using Vickers surface microhardness (SMH), environmental scanning electron microscopy (ESEM), and energy dispersive X-ray spectroscopy (EDX). Results demonstrate that demineralization produced the expected decline in enamel SMH and mineral content, while all treatment groups produced partial to near-complete recovery;

Tianjin Daxue Xuebao (Ziran Kexue yu Gongcheng Jishu Ban)/
Journal of Tianjin University Science and Technology
ISSN (Online):0493-2137
E-Publication: Online Open Access
Vol: 59 Issue: 07:2026
DOI: 10.5281/zenodo.21412229

the greatest improvements in mechanical and compositional measures occurred when β-TCP was added to the NaF + arginine formulation. Caries initiation is driven by loss of calcium and phosphorus from enamel, producing subsurface, reversible initial carious lesions (ICL) that are amenable to non-invasive remineralization (Aziz, 2021). Fluoride remains a cornerstone of remineralization therapy, but its optimal effect depends on the availability of calcium and phosphate ions to form stable fluorapatite and to favor surface and subsurface repair (Iwawaki *et al.,* 2024; Li *et al.,* 2014). Consistent with these mechanistic insights, the NaF-only group (500 ppm) in our study produced a measurable increase in SMH and fluoride uptake versus demineralized controls, likely reflecting surface precipitation of calcium fluoride–like deposits and partial incorporation into apatite (Sivapriya *et al.,* 2017). However, NaF alone yielded less recovery than combinations that supplied additional calcium/phosphate or promoted their targeted delivery.

Arginine was selected to augment fluoride's performance because it can chelate and localize mineral ions and promote favorable conditions for remineralization while maintaining biocompatibility at 2% concentration (Bijle *et al.,* 2018; Bijle *et al.,* 2020). In line with prior reports (Cheng *et al.,* 2015; Yu *et al.,* 2016), the NaF + 2% arginine group produced greater SMH gains and higher surface fluoride levels than NaF alone. The observed synergy can be explained by arginine's dual interaction with mineral ions: it forms complexes (Arg–Ca–F2) that increase localized supersaturation and favor crystal growth within porous enamel, while gradually releasing fluoride under acidic challenge to sustain protection (Bijle *et al.,* 2020). CCK-8 cytotoxicity data from the literature support 2% arginine as an effective, non-cytotoxic concentration compared with higher, cytotoxic levels (Bijle *et al.,* 2020).

Addition of a calcium/phosphate source further potentiated remineralization. Nano β-TCP derived from cuttlefish bone was chosen for its low cost, biocompatibility, and favorable ion-release profile (Abd-elmonsif and Gamal, 2024; Hemagaran and Neelakantan, 2014). The NaF + arginine + 1% β-TCP group produced the highest SMH values and EDX-measured Ca and P recovery that approached sound enamel levels, as well as the highest fluoride content (though not significantly different from NaF + arginine alone). These findings mirror prior demonstrations that combining fluoride with bioavailable calcium/phosphate sources yields more complete remineralization and formation of more acid-resistant fluorapatite (Hamba *et al.,* 2020; Hou *et al.,* 2021). Nanotechnology likely contributed to the improved outcomes by increasing surface area and reactivity, facilitating deeper ion penetration into subsurface lesions, and promoting formation of a homogeneous, tightly packed mineral layer (Elmarsafy, 2024).

Methodological choices strengthened the clinical relevance and internal validity of our findings. Intact premolars extracted for orthodontic reasons provided ethically obtainable, sound human enamel with sufficient buccolingual width to allow split-tooth design and minimize intersample variability (Mahtani and Jain, 2020; Jaswal *et al.,* 2025). Young donor teeth, which may have relatively porous, immature enamel, are particularly relevant to early lesion remineralization research (Majithia *et al.,* 2016). Careful specimen preparation stereomicroscope screening to exclude caries or cracks (Gumus *et al.,* 2020),

Tianjin Daxue Xuebao (Ziran Kexue yu Gongcheng Jishu Ban)/
Journal of Tianjin University Science and Technology
ISSN (Online):0493-2137
E-Publication: Online Open Access
Vol: 59 Issue: 07:2026
DOI: 10.5281/zenodo.21412229

hand scaling to avoid surface abrasion caused by ultrasonic scaling (Kumari *et al.,* 2023), and use of fluoride-free medium-grit paste reduced potential confounders from extrinsic fluoride or iatrogenic surface alteration (Aziz, 2021). Storage in isotonic 0.9% saline at 4 °C with daily renewal limited ion leaching or organic interactions associated with distilled water or milk, respectively, preserving baseline mineral composition (Udoye *et al.,* 2012; Obied and Saleem, 2022; Atia *et al.,* 2023).

Artificial lesion creation used an acetic acid–based demineralizing solution at pH 4.4 for 96 h, producing chalky incipient lesions comparable to natural caries while avoiding overly aggressive acid protocols (Yu *et al.,* 2017; Mashhour *et al.,* 2023; Milanović *et al.,* 2023). A pH-cycling regime was employed to simulate the dynamic oral environment of alternating demineralization and remineralization phases; specimens underwent eight days of cycles with 2-hour daily demineralization and 22-hour artificial saliva exposure, and remineralizing solutions were applied three times daily (Queiroz *et al.,* 2008; Delbem *et al.,* 2006; Ten Cate *et al.,* 2008). Daily replacement of immersion media limited depletion of critical ions and maintained consistent experimental conditions (Konagala *et al.,* 2020; Mashhour *et al.,* 2023).

Choice of assessment techniques supported robust interpretability. Vickers microhardness testing (100 g for 10 s) provided a rapid, reliable, and non-destructive mechanical measure reflecting enamel resistance to indentation and wear (Aziznezhad *et al.,* 2017; Petrík, 2011). ESEM allowed morphological assessment of hydrated, uncoated samples and revealed progressive improvement from the honeycombed porosities of demineralized enamel to smoother, more compact surfaces in treated groups, with the tri-component group most closely resembling sound enamel (Hegde and Moany, 2012; Orilisi *et al.,* 2025; Nicolae *et al.,* 2011). EDX quantified elemental recovery: demineralized enamel showed substantial losses in Ca and P that were partially restored after treatment, with the β-TCP group achieving near-baseline Ca and P percentages and the highest surface fluoride uptake, consistent with comprehensive mineral replenishment (El Hagry *et al.,* 2021; Konagala *et al.,* 2021).

Limitations include the inherent constraints of in vitro models: absence of salivary flow, pellicle formation, biofilm dynamics, and mechanical wear may influence ion availability and lesion progression in vivo. Although the pH-cycling model and artificial saliva sought to mimic oral conditions, clinical trials are needed to confirm efficacy, safety, substantivity, and long-term outcomes in situ. Additionally, while EDX provides surface elemental proportions, it does not directly reveal subsurface mineral distribution; complementary transverse microradiography or cross-sectional nanoindentation could further characterize lesion depth and mineral gradients. Finally, the biogenic source and nanoparticle characteristics of cuttlefish-derived β-TCP (particle size distribution, crystallinity, and possible organic residues) warrant further physicochemical characterization and standardized production to ensure reproducibility and regulatory compliance. In conclusion, combining 500 ppm NaF with 2% arginine enhanced fluoride uptake and enamel surface microhardness compared with NaF alone, and adding 1% biogenic nano β-TCP produced the most pronounced restorative effect, achieving

Tianjin Daxue Xuebao (Ziran Kexue yu Gongcheng Jishu Ban)/
Journal of Tianjin University Science and Technology
ISSN (Online):0493-2137
E-Publication: Online Open Access
Vol: 59 Issue: 07:2026
DOI: 10.5281/zenodo.21412229

near-sound enamel mineral content and morphology. These results support a synergistic remineralization strategy in which arginine improves ion localization and delivery while β-TCP supplies bioavailable calcium and phosphate to complement fluoride's action potentially enabling effective remineralization at lower fluoride concentrations. Future work should include in situ and clinical trials, mechanistic studies of Arg–Ca–F complexes in enamel, and standardized characterization of biogenic nano β-TCP for translation into safe, effective, and environmentally conscious preventive dental products.

Limitation: There are some limitations of the study: 1) The collection of teeth that met the inclusion criteria. 2) Very expensive tests (VMHT), (ESEM), and (EDX).3) Artificial saliva, arginine solution, and nano biogenic-derived β-TCP required experienced scientific laboratory support. 4) The multi-stage pH-cycling protocol and repeated treatment applications required extensive time and effort.

CONCLUSION

The present in vitro study confirmed that the employed demineralization protocol reliably produced artificial enamel lesions, demonstrated by a significant decrease in surface microhardness and characteristic morphological alterations on SEM. All tested remineralizing agents promoted recovery of demineralized enamel, evidenced by increases in surface microhardness, smoother surface morphology, and elevated calcium and phosphorus content. Notably, arginine enhanced fluoride uptake, and the combined application of fluoride, arginine, and biogenic β-tricalcium phosphate produced the greatest remineralization effect, yielding the highest microhardness values, fluoride uptake, and Ca:P ratio. These results indicate a synergistic interaction among fluoride, arginine, and biogenic β-TCP in promoting enamel repair and suggest that their combined use may offer superior therapeutic benefit for remineralization strategies.

Recommendations:

Future in vivo studies are needed to confirm the remineralization potential of fluoride, arginine, and β-tricalcium phosphate under real oral conditions. A polymicrobial pH-cycling model should be used to evaluate arginine's antibacterial effects and better simulate oral biofilm dynamics and acid challenge. Additionally, formulation and testing of a toothpaste combining fluoride, arginine, and β-tricalcium phosphate is recommended, as a toothpaste vehicle promotes sustained contact with the tooth surface and enhances patient compliance. Together, these approaches will validate laboratory findings and inform development of an effective, clinically applicable anti-caries dentifrice.

References

1) **Abd-elmonsif, N., & Gamal, S. (2024).** 'Potential remineralizing effect of cuttlefish bone and eggshell Powder's on demineralized human enamel: an in vitro study'. Pediatric Dental Journal, 34(3), pp. 122-128. doi.10.1016/j.pdj.2024.08.003.

2) **Abdslam, A., Farag, M., Mahfouz, S. (2022).** 'Evaluation of the Effect of Two Different Concentration of Arginine on Fluoride Uptake by Demineralized Enamel Surfaces: in vitro study'. Dental Science Updates, 3(2), pp .199-208. doi.10.21608/dsu.2022.117363.1098.

Tianjin Daxue Xuebao (Ziran Kexue yu Gongcheng Jishu Ban)/
Journal of Tianjin University Science and Technology
ISSN (Online):0493-2137
E-Publication: Online Open Access
Vol: 59 Issue: 07:2026
DOI: 10.5281/zenodo.21412229

3) **Al-Qahtani, A., Tulbah, H., Binhasan, M., Shabib, S., Al-Aali, K., Alhamdan, M., & Abduljabbar, T. (2022).** 'Influence of concentration levels of β-tricalcium phosphate on the physical properties of a dental adhesive'. *Nanomaterials*, *12*(5), 853. doi.10.3390/nano12050853.

4) **Arifa, M., Ephraim, R., & Rajamani, T. (2019).** 'Recent Advances in Dental Hard Tissue Remineralization: A Review of Literature'. *International Journal of Clinical Pediatric Dentistry*, *12*(2), pp. 139–144. doi:10.5005/jp-journals-10005-1603.

5) **Atia, N., El-Nemr, R., & Abo-Elsoud, A. (2023).** 'Effect of lactoferrin on enamel characteristics of primary and permanent teeth: an in-vitro study'. BMC Oral Health, pp. 23(1), 993. doi: 10.1186/s12903-023-03709-1.

6) **Aziz, M. (2021).** 'Changes in mineral density and nanomechanical properties of enamel white spot lesions by dentifrices with different active ingredients for remineralisation-an in vitro study' (Doctoral dissertation, University of Otago).

7) **Aziznezhad, M., Alaghemand, H., Shahande, Z., Pasdar, N., Bijani, A., Eslami, A., & Dastan, Z. (2017).** 'Comparison of the effect of resin infiltrant, fluoride varnish, and nano-hydroxy apatite paste on surface hardness and streptococcus mutans adhesion to artificial enamel lesions'. Electronic physician, 9(3), pp. 3934–3942. doi.org/10.19082/3934.

8) **Bijle, M., Ekambaram, M., Lo, E., & Yiu, C. (2018).** 'The combined enamel remineralization potential of arginine and fluoride toothpaste'. *Journal of Dentistry*, *76*, pp.75–82.doi.10.1016/j.jdent.2018.06.009.

9) **Bijle, M., Ekambaram, M., Lo, E., & Yiu, C. (2020).** 'The enamel remineralization potential of fluoride varnishes containing arginine'. *Journal of Dentistry*, *99*, p.103411.doi.10.1016/j.jdent.2020.103411.

10) **Bijle, M., Tung, L., Wong, J., Ekambaram, M., Lo, E., & Yiu, C. (2019).** 'Enhancing the remineralization potential of child formula dentifrices: An in vitro study'. Journal of Clinical Pediatric Dentistry, 43(5), pp.337-344. doi:10.17796/1053-4625-43.5.6.

11) **Cury, J., Ricomini-Filho, A., Berti, F., & Tabchoury, C. (2019).** 'Systemic Effects (Risks) of Water Fluoridation'. Brazilian Dental Journal, 30(5), pp. 421–428. doi.10.1590/0103-6440201903124.

12) **Dalal, M., & Clark, M. (2019).** 'Pediatric oral health: Fluoride use recommendations'. *Contemporary Pediatric Journal*, 36(2).

13) **Delbem, A., Bergamaschi, M., Sassaki, K., & Cunha, R.(2006).** 'Effect of fluoridated varnish and silver diamine fluoride solution on enamel demineralization: pH-cycling study. *Journal of Applied Oral Science*, 14(2), pp.88–92.doi.10.1590/s1678-77572006000200005.

14) **El Hagry, B., El-Baz, G., & Abo El Soud, A. (2021).** 'Comparative Evaluation of Remineralizing Effect of Casein Phosphopeptide–Amorphous Calcium Phosphate Fluoride and Silver Diamine Fluoride on Demineralized Enamel Surfaces: An In Vitro Study '. *Dental Science Updates*, *2*(2), pp. 135-143.

15) **Elmarsafy S. (2024).** 'A Comprehensive Narrative Review of Nanomaterial Applications in Restorative Dentistry: Demineralization Inhibition and Remineralization Applications' . *Cureus*, *16*(4), e58544.doi.10.7759/cureus.58544.

16) **Featherstone J. (2009).** 'Remineralization, the natural caries repair process- the need for new approaches'. Advances in Dental Research, 21(1), pp.4–7. doi.10.1177/0895937409335590

17) **Gumus, H., Aydınbelge, M., & Sonmez, H. (2020).** 'Evaluation of the Efficacy of Different Remineralizing Agents on Artificial Early Enamel Lesions of Primary Teeth: An in vitro Study'. Journal of Advanced Oral Research, 11(2), pp .180-188. doi: 10.1177/2320206820919664.

18) **Hamba, H., Nakamura, K., Nikaido, T., Tagami, J., & Muramatsu, T. (2020).** 'Remineralization of enamel subsurface lesions using toothpaste containing tricalcium phosphate and fluoride: an in vitro μCT analysis'. *BMC Oral Health*, *20*(1), P. 292. doi.10.1186/s12903-020-01286-1.

Tianjin Daxue Xuebao (Ziran Kexue yu Gongcheng Jishu Ban)/
Journal of Tianjin University Science and Technology
ISSN (Online):0493-2137
E-Publication: Online Open Access
Vol: 59 Issue: 07:2026
DOI: 10.5281/zenodo.21412229

19) **Hamdy, T., 2024.** 'Evaluation of flexural strength, impact strength, and surface microhardness of self-cured acrylic resin reinforced with silver-doped carbon nanotubes'. BMC Oral Health, 24(1), p.151. doi.10.1186/s12903-024-03909-3.

20) **Hegde, M. , & Moany, A. (2012).** 'Remineralization of enamel subsurface lesions with casein phosphopeptide-amorphous calcium phosphate: A quantitative energy dispersive X-ray analysis using scanning electron microscopy: An: in vitro: study'. *Journal of Conservative Dentistry*, 15(1), pp. 61-67. doi.10.4103/0972-0707.92609.

21) **Hemagaran, G., & Neelakantan, P. (2014).** ' Remineralization of the tooth structure-the future of dentistry'. *International Journal of Pharm Tech Research,* 6 (2), pp. 487-493.

22) **Hou, P., Lee, C., Ou, K., Lan, W.-, Chuo, Y., Lin, H., Chao, H., Huang, B., Saito, T., Tsai, H., Yang, T., Walinski, C. , & Ruslin, M. (2021).** ' Calcium Release from Different Toothpastes after the Incorporation of Tricalcium Phosphate and Amorphous Calcium Phosphate'. Applied Sciences, 11(4), p. 1848. doi.10.3390/app11041848.

23) **Iwawaki, R., Horie, T., Alhotan, A., Nagatsuka, Y., Sakuma, K., Yoshihara, K., & Tsujimoto, A. (2024).** ' Effect of Fluoride Varnishes on Demineralization and Acid Resistance in Subsurface Demineralized Lesion Models'. Journal of Functional Biomaterials, 15(12), p.380. doi.10.3390/jfb15120380.

24) **Jaswal, A., Attur, S., Patel, A., Sarathy, N., Visavadiya, A., & Patel, N. (2025).** Odontometric Study of Premolars: A Convenient Method for Gender Determination. International Board, 19(3), 69.

25) **Kabir, H., Gupta, A. , & Tripathy, S. (2019).** 'Fluoride and human health: Systematic appraisal of sources, exposures, metabolism, and toxicity'. *Critical Reviews in Environmental Science and Technology*, *50*(11), pp. 1116–1193. doi.10.1080/10643389.2019.1647028

26) **Kashyap, S., Sankannavar, R., & Madhu, G. (2021).** 'Fluoride sources, toxicity and fluorosis management techniques–A brief review'. Journal of Hazardous Materials Letters, 2, p. 100033. doi.10.1016/j.hazl.2021.100033.

27) **Konagala, R. K., Mandava, J., Anwarullah, A., Uppalapati, L. V., Karumuri, S., & Angadala, P. L. (2021).** 'Synergistic effect of arginine on remineralization potential of fluoride varnish and nanohydroxyapatite on artificial caries lesions: an in vitro study'. *The Journal of Contemporary Dental Practice*, *21*(9), pp. 1048-1053. doi. 10.5005/jp-journals-10024-2915.

28) **Konagala, R., Mandava, J., Anwarullah, A., Uppalapati, L., Karumuri, S., & Angadala, P. (2020).** 'Synergistic effect of arginine on remineralization potential of fluoride varnish and nanohydroxyapatite on artificial caries lesions': an *in vitro* study'. *The Journal of Contemporary Dental Practice*, *21(9)*, pp. 1048-1053. doi:33568594.

29) **Kumari, N., Johnson, L., Yadav, H., Das, A., Umrao, B., & Gera, R. (2023).** 'Effect of Hand and Ultrasonic Scaling-Root Planing Methods on Tooth Surface Topography: An In-Vitro Atomic Force Microscopy Study'. Cureus, 15(10), e46925. doi.10.7759/cureus.46925.

30) **Kuriki, N., Asahi, Y., Okamoto, M., Noiri, Y., Ebisu, S., Machi, H., Suzuki, M., & Hayashi, M. (2024).** 'Synergistic effects of arginine and fluoride on human dental biofilm control'. Journal of Dentistry, 149, p. 105307. doi.10.1016/j.jdent.2024.105307.

31) **Li, X., Wang, J., Joiner, A., & Chang, J. (2014).** 'The remineralisation of enamel: a review of the literature'. Journal of Dentistry, 42(1), pp.12-20. doi.10.1016/S0300-5712(14)50003-6.

32) **Limeback, H., Enax, J., Meyer, F. (2023).** 'Improving Oral Health with Fluoride-Free Calcium-Phosphate-Based Biomimetic Toothpastes: An Update of the Clinical Evidence'. Biomimetics, 8(4), P. 331. doi.10.3390/biomimetics8040331

Tianjin Daxue Xuebao (Ziran Kexue yu Gongcheng Jishu Ban)/
Journal of Tianjin University Science and Technology
ISSN (Online):0493-2137
E-Publication: Online Open Access
Vol: 59 Issue: 07:2026
DOI: 10.5281/zenodo.21412229

33) **Madhukumar, K., Varma, H. , Komath, M., Elias, T. , Padmanabhan, V., & Nair, C. (2007).** 'Photoluminescence and thermoluminescence properties of tricalcium phosphate phosphors doped with dysprosium and europium'. *Bulletin of Materials Science*, *30*(5), 527-534. doi. 10.7759/cureus.58544.

34) **Mahtani, A., & Jain, R. K. (2020).** 'Frequency of premolar teeth extractions for orthodontic treatment'. Bioinformation, 16(12), pp. 1080–1087. doi.10.6026/973206300161080.

35) **Majithia, U., Venkataraghavan, K., Choudhary, P., Trivedi, K., Shah, S., & Virda, M. (2016).** Comparative evaluation of application of different fluoride varnishes on artificial early enamel lesion: An in vitro study. Indian journal of dental research: official publication of Indian Society for Dental Research, 27(5), 521–527. doi.10.4103/0970-9290.195642.

36) **Mashhour, A., Allam, G., & Wassel, M. (2023).** 'Comparative evaluation of prevention of demineralization of artificial enamel caries treated with two fluoride varnishes and 38% SDF in primary teeth: an in vitro study'. *BMC oral health*, *23*(1), p.110. doi.10.1186/s12903-023-02799-1.

37) **Mehdikhani, B., & Borhani, G. (2014)**. 'Densification and mechanical behavior of β-tricalcium phosphate bioceramics'. *International letters of chemistry, Physics and Astronomy*, *17*.

38) **Meyer, F., Enax, J., Amaechi, B. , Limeback, H., Fabritius, H., Ganss, B., ... & Paszynska, E. (2022).** 'Hydroxyapatite as remineralization agent for children's dental care'. Frontiers in Dental Medicine, 3, e859560. doi.10.3389/fdmed.2022.859560.

39) **Milanović, M., Mandinić, Z., Juloski, J., Dimitrijević, M., Miličić, B., Anđelski-Radičević, B.,& Beloica, M. (2023).** 'Effect of different demineralizing solutions and different exposing times on artificial initial caries lesion formation–an in vitro study'. Srpski Arhiv za Celokupno Lekarstvo, 151(11-12), pp. 652-657. doi.10.2298/SARH221228095M.

40) **Nicolae, C., Hîncu, M. , & Amariei, C. (2011).** 'Scanning electron microscopic observation of morphological modifications produced by Fluorostom on enamel surface'. *Romanian Journal of Morphology and Embryology*, *52*(4), pp.1255-1259.

41) **Obeid, R., & Saleem, M. (2022).** 'Efficacy of several forms of storage medium on avulsed teeth's enamel surface roughness: an in vitro study'. *Journal of Research in Medical and Dental Science*, 10(4), pp.92-7.

42) **Orilisi, G., Monterubbianesi, R., Vitiello, F., Tosco, V., Gatto, M. , Mengucci, P., & Orsini, G. (2025).** 'Time-Effect Comparative Evaluation of Three Remineralizing Agents on Artificial Enamel Lesions: A SEM-EDX In Vitro Study'. Journal of Clinical Medicine, 14(20), p.7389. doi.10.3390/jcm14207389.

43) **Pang, B., Xian, J., Chen, J., Ng, L., Li, M., Zhao, G., E, Y., Wang, X., Cao, X., Zhang, C., Zhang, M., & Liu, C. (2024).** 'Cuttlefish Bone-Derived Calcium Phosphate Bioceramics Have Enhanced Osteogenic Properties'. Journal of Functional Biomaterials, 15(8), p.212. doi.org/10.3390/jfb15080212.

44) **Pecharsky, V. & Zavalij, P. (2003).** 'Fundamentals of powder diffraction and structural characterization of materials'. Boston, MA: Springer US.

45) **Petrík, J. (2011).** 'The influence of the load on the quality of microhardness measurement'. *Acta Metallurgica Slovaca*, 17(3), pp. 207-216.

46) **Prasad, J., Bhojraj, N., Shanbhog, R., & Ashwini, K. (2023).** 'Combined remineralizing effect of arginine and fluoride on artificially demineralized human primary dentin evaluated using quantitative light induced fluorescence'. J*ournal of Indian Society of Pedodontics and Preventive Dentistry*, 41(1), pp. 63-69. doi: 10.4103/jisppd.jisppd_107_23.

Tianjin Daxue Xuebao (Ziran Kexue yu Gongcheng Jishu Ban)/
Journal of Tianjin University Science and Technology
ISSN (Online):0493-2137
E-Publication: Online Open Access
Vol: 59 Issue: 07:2026
DOI: 10.5281/zenodo.21412229

47) **Queiroz, C., Hara, A., Paes Leme, A., & Cury, J. (2008).** 'pH-cycling models to evaluate the effect of low fluoride dentifrice on enamel de- and remineralization'. *Brazilian Dental Journal*, *19*(1), pp. 21–27. doi.10.1590/s0103-64402008000100004.

48) **Salinovic, I., Schauperl, Z., Marcius, M., & Miletic, I. (2021).** 'The Effects of Three Remineralizing Agents on the Microhardness and Chemical Composition of Demineralized Enamel'. *Materials*, *14*(20), p. 6051. doi.10.3390/ma14206051.

49) **Seyedlar, R. M., Rezvani, M., Barari, S., Imani, M., Nodehi, A., & Atai, M. (2019).** 'Synthesis of plate-like β-tricalcium phosphate nanoparticles and their efficiency in remineralization of incipient enamel caries'. *Progress in Biomaterials*, *8*(4), pp. 261–276. doi.10.1007/s40204-019-00126-y.

50) **Sivapriya, E., Sridevi, K., Periasamy, R., Lakshminarayanan, L., & Pradeepkumar, A. R. (2017).** 'Remineralization ability of sodium fluoride on the microhardness of enamel, dentin, and dentinoenamel junction: An *in vitro* study'. *Journal of Conservative Dentistry*, *20*(2), pp. 100–104. doi.10.4103/JCD.JCD_353_16.

51) **Toumba, K., Twetman, S., Splieth, C., Parnell, C., van Loveren, C., Lygidakis, N. (2019).** 'Guidelines on the use of fluoride for caries prevention in children: an updated EAPD policy document'. *European Archives of Paediatric Dentistry: Official Journal of the European Academy of Paediatric Dentistry*, *20*(6), pp. 507–516.doi.10.1007/s40368-019-00464-2.

52) **Udoye, C. I., Jafarzadeh, H., & Abbott, P. V. (2012).** 'Transport media for avulsed teeth: a review'. Australian Endodontic Journal, 38(3), pp. 129-136.doi.10.1111/j.1747-4477.2012.00356.x.

53) **Wierichs, R. J., Stausberg, S., Lausch, J., Meyer-Lueckel, H., & Esteves-Oliveira, M. (2018).** 'Caries-Preventive Effect of NaF, NaF plus TCP, NaF plus CPP-ACP, and SDF Varnishes on Sound Dentin and Artificial Dentin Caries in vitro'. *Caries Research*, *52*(3), pp.199–211. doi.10.1159/000484483.

54) **Wong, M., Zhang, R., Luo, B., Glenny, A., Worthington, H., & Lo, E. (2024).** Topical fluoride as a cause of dental fluorosis in children'. 'The Cochrane Database of Systematic Reviews, 6(6), CD007693. doi.10.1002/14651858.CD007693.pub3.

55) **Yu, O. , Zhao, I. , Mei, M. , Lo, E., & Chu, C.(2017).** 'A Review of the Common Models Used in Mechanistic Studies on Demineralization-Remineralization for Cariology Research'. *Dentistry Journal*, *5*(2), P.20. doi.10.3390/dj5020020.

56) **Yu, P., Arola, D. D., Min, J., Yu, D., Xu, Z., Li, Z., & Gao, S. (2016).** 'Investigation on the remineralization effect of arginine toothpaste for early enamel caries: nanotribological and nanomechanical properties'. *Journal of Physics D: Applied Physics*, *49*(43), p. 435401. doi.10.1088/0022-3727/49/43/435401.

57) **Zheng, F., Adiatman, M., Chu, C., Crystal, Y., Featherstone, J., Hoang, T., Kim, B., Ogawa, H., Pitiphat, W., Kadir, R., Wong, M., & Zheng, S. (2024).** 'Recommendations on Topical Fluoride Usage for Caries Management in East Asia'. *International Dental Journal*, *74*(5), pp. 910–916. doi.10.1016/j.identj.2024.04.016.